

AD-A129 568

LABORATORY STUDY OF SPACE SHUTTLE PROPELLANT TANK ICING 1/1  
(U) AEROSPACE CORP EL SEGUNDO CA AEROPHYSICS LAB

J F BOTT ET AL 17 MAY 83 TR-0083(3464-02-1)

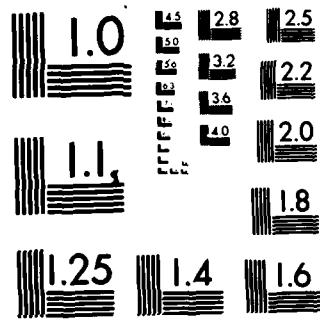
UNCLASSIFIED

SD-TR-83-32 F04701-82-C-0083

F/G 22/2

NL


END  
DATE  
FILMED  
DTIC



MICROCOPY RESOLUTION TEST CHART  
NATIONAL BUREAU OF STANDARDS-1963-A

ADA129505

# Laboratory Study of Space Shuttle Propellant Tank Icing

J. F. BOTT, D. H. ROSS,  
D. J. SPENCER, and J. S. WHIFFER  
Aerophysics Laboratory  
Laboratory Operations  
The Aerospace Corporation  
El Segundo, Calif. 90245

17 May 1983

APPROVED FOR PUBLIC RELEASE  
DISTRIBUTION UNLIMITED

**DTIC**  
A

DTIC FILE COPY


Prepared for  
SPACE DIVISION  
AIR FORCE SYSTEMS COMMAND  
Los Angeles Air Force Station  
P.O. Box 92960, Worldway Postal Center  
Los Angeles, Calif. 90009

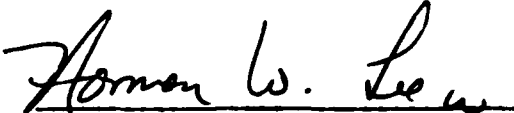
83 06 20 029

This report was submitted by The Aerospace Corporation, El Segundo, CA 90245, under Contract No. F04701-82-C-0083 with the Space Division, P.O. Box 92960, Worldway Postal Center, Los Angeles, CA 90009. It was reviewed and approved for The Aerospace Corporation by W. P. Thompson, Jr., Director, Aerophysics Laboratory. 2nd Lt Eva Allen, SD/YCR, was the Air Force project officer.

This report has been reviewed by the Public Affairs Office (PAS) and is releasable to the National Technical Information Service (NTIS). At NTIS, it will be available to the general public, including foreign nationals.

This technical report has been reviewed and is approved for publication. Publication of this report does not constitute Air Force approval of the report's findings or conclusions. It is published only for the exchange and stimulation of ideas.

  
Eva Allen, 2nd Lt, USAF  
Project Officer

  
Norman W. Lee, Jr., Colonel, USAF  
Commander, Det 1, AFSTC

UNCLASSIFIED

SECURITY CLASSIFICATION OF THIS PAGE (When Data Entered)

REPORT DOCUMENTATION PAGE		READ INSTRUCTIONS BEFORE COMPLETING FORM
1. REPORT NUMBER SD-TR-83-32	2. GOVT ACCESSION NO.	3. RECIPIENT'S CATALOG NUMBER
4. TITLE (and Subtitle) LABORATORY STUDY OF SPACE SHUTTLE PROPELLANT TANK ICING		5. TYPE OF REPORT & PERIOD COVERED
		6. PERFORMING ORG. REPORT NUMBER TR-0083(3464-02)-1
7. AUTHOR(s) J. F. Bott, D. H. Ross, D. J. Spencer, and J. S. Whittier		8. CONTRACT OR GRANT NUMBER(s) F04701-82-C-0083
9. PERFORMING ORGANIZATION NAME AND ADDRESS The Aerospace Corporation El Segundo, California 90245		10. PROGRAM ELEMENT, PROJECT, TASK AREA & WORK UNIT NUMBERS
11. CONTROLLING OFFICE NAME AND ADDRESS Space Division Air Force Systems Command Los Angeles, California 90009		12. REPORT DATE 17 May 1983
		13. NUMBER OF PAGES 34
14. MONITORING AGENCY NAME & ADDRESS (if different from Controlling Office)		15. SECURITY CLASS. (of this report) Unclassified
		15a. DECLASSIFICATION/DOWNGRADING SCHEDULE
16. DISTRIBUTION STATEMENT (of this Report)  Approved for public release; distribution unlimited.		
17. DISTRIBUTION STATEMENT (of the abstract entered in Block 20, if different from Report)		
18. SUPPLEMENTARY NOTES		
19. KEY WORDS (Continue on reverse side if necessary and identify by block number) Space shuttle VAFB launch site Ice formation Sprayed-on foam insulation (SOFI) Insulation Cryogenic fuel tanks		
20. ABSTRACT (Continue on reverse side if necessary and identify by block number) Small-scale experiments have been performed with SOFI (sprayed-on-foam-insulation) panels shaved to 0.5- and 0.9-in. thicknesses. The rear sides of the SOFI panels were cooled to LN <sub>2</sub> temperatures; the front sides were exposed to an environmental chamber with controlled temperature and humidity. The measured rates of frost formation and the observed surface temperatures are consistent with predictions obtained with a simple heat balance model. The measured frost densities, on the other hand, were less than 6 lb/ft <sup>3</sup> , much		

DD FORM 1473 (FACSIMILE)

UNCLASSIFIED

SECURITY CLASSIFICATION OF THIS PAGE (When Data Entered)

UNCLASSIFIED

SECURITY CLASSIFICATION OF THIS PAGE(When Data Entered)

19. KEY WORDS (Continued)

*Cubic Centimeter*  
*Cubic feet*

20. ABSTRACT (Continued)

lower than those predicted by the University of Dayton Research Institute frost formation model. In a worst-case test, hard ice was observed when water was dripped down the surface of a 0.5-in.-thick, LN<sub>2</sub>-chilled SOFI panel. A preliminary study of solar melting produced little rundown or ice. Frost densities of less than 0.1 g/cm<sup>3</sup> (6 lb/ft<sup>3</sup>) were obtained, except in the test in which water was dripped onto the surface.

Validation by the present experiments of predictions based on a heat balance model applies only to natural convection in the laminar flow regime. A large fraction of the flow on the space shuttle fuel tank will be in the turbulent regime because of the height of the tank. Larger-scale tests would be required to validate the turbulent heat transfer coefficients.

↑

UNCLASSIFIED

SECURITY CLASSIFICATION OF THIS PAGE(When Data Entered)

CONTENTS

I. INTRODUCTION..... 5

II. APPARATUS..... 7

III. PROCEDURE..... 9

IV. RESULTS..... 11

    A. Preliminary Tests 1 through 6..... 11

    B. Shaved Panel--0.5 in. Thick..... 11

    C. Shaved Panel--0.9 in. Thick..... 14

    D. Effect of Simulated Solar Radiation..... 18

V. HEAT BALANCE MODEL PREDICTIONS..... 21

VI. DISCUSSION..... 25

VII. SUMMARY..... 33

REFERENCES..... 35

APPENDIX. HEAT BALANCE MODEL..... 37



Date		Per
DTIC	DTIC	<input checked="" type="checkbox"/>
DTIC	DTIC	<input type="checkbox"/>
DTIC	DTIC	<input type="checkbox"/>
Classification/		
Availability Codes		
Availability Codes		
Special		
A		

## FIGURES

1.	Frost mass and thickness measurements for 0.5-in. SOFI in test 12.....	12
2.	Surface temperature of 0.5-in. SOFI in test 12.....	13
3.	Ice formation in test 14.....	16
4.	Photograph of lamp arrangement for tests 23 and 24.....	19
5.	Calculated frost accumulation rates versus measured frost accumulation rates.....	26
6.	Measured frost accumulation rates versus water-vapor partial pressure ( $P_{amb} - P_{surf}$ ).....	27
7.	Frost density versus calculated surface temperatures.....	29
8.	Thermal conductivities of frost deduced from tests 8 through 13.....	32

## TABLES

1.	Experimental Data for 0.5-in. Panel.....	15
2.	Experimental Data for 0.9-in. Panel.....	17
3.	Comparison of Experimental and Calculated Values of Frost Growth Rates and Surface Temperatures for Tests 8 through 13.....	22
4.	Comparison of Experimental and Calculated Values of Frost Growth Rates and Surface Temperatures for Tests 18 through 22.....	23



## I. INTRODUCTION

Operation of the Space Transportation System (STS) from Vandenberg Air Force Base (VAFB), rather than from the warmer Kennedy Space Center (KSC), has raised the question of whether ice will form on the foam-insulated external tank containing cryogenic propellants. Ice accumulation and, in particular, falling ice loosened by the launch represent a potential hazard to the orbiter; a launch will be postponed for certain predetermined ice conditions. The existing mathematical model<sup>1</sup> of heat transfer and ice formation predicts that launches would be delayed more often at VAFB than at KSC.

The purpose of this study was to obtain subscale experimental data to validate some portions of the mathematical model. In addition, the present study served as a "pathfinder" for larger-scale experiments.

Predictions by the mathematical model indicate that, for certain air temperature and humidity conditions that depend on the wind velocity, cloud cover, time of day, and insulation thickness, the surface temperature of the external propellant tank can fall below the freezing point of water. Freezing occurs most readily when the air is still (no forced convection) and only natural convection and radiation warm the surface of the tank. For this reason, we decided to test a simulated section of the external propellant tank (ET) in a controlled environmental chamber under the still conditions of natural convection. We controlled temperature and humidity, and measured the buildup of frost mass and thickness at intervals during tests lasting up to 6 hr. Surface temperatures were also monitored. The measured frost accretion (accumulation) rates and surface temperatures were compared with the predictions of a simplified heat balance equation.

## II. APPARATUS

The tests were conducted in an environmental chamber measuring 6 x 6 x 11 ft that was lined on the inside with foam insulation. The chamber has a built-in air conditioner/blower in the ceiling. However, when the air conditioner was operated for several hours under high-humidity conditions, the coils would frost over, reducing the ability of the air conditioner to cool the chamber. Consequently, we placed two large-area heat exchangers in the chamber to permit cooling without excessive moisture extraction from the air. The heat exchangers were cooled with liquid nitrogen (LN<sub>2</sub>)-chilled water-glycol mixtures to temperatures a few degrees above freezing, i.e., near 32 to 35°F. The humidity in the chamber could be controlled independently with three residential humidifiers to nearly 100 percent relative humidity (RH).

Test panels were constructed to simulate a section of the external tank. They were made by attaching a 36 x 16-in. test sample of sprayed-on foam insulation (SOFI) to one side of a 1-in.-thick aluminum frame. The SOFI test samples were obtained from Martin-Michoud and were CPR 488 sprayed onto the 1/8-in. aluminum sheet. The back side of the frame was covered with a sheet of 1/8 x 36 x 16-in. aluminum. The aluminum sheets were fastened to the frame with machine screws and sealed with RTV silicone cement. The test panels were designed to hold LN<sub>2</sub>, and Styrofoam insulation was placed on all exposed aluminum surfaces. The SOFI samples had an original thickness of between 1-1/2 and 1-3/4 in. We shaved one sample to 0.5-in. thickness for the first test series (tests 7-17) and another sample to 0.9 in. for the second series (tests 18-24). The SOFI was shaved to obtain faster frosting rates and to facilitate obtaining frost samples from the smoother surface.

The panel was filled with LN<sub>2</sub> through a 1/2-in. insulated line from a commercial LN<sub>2</sub> tank. Nitrogen gas boil off was exhausted through a line to the outside of the building. The pressure in the panel was monitored with a Heise Bourdon gage, and the LN<sub>2</sub> flow rate was controlled to prevent a pressure greater than about 1 psig. A glass dipstick containing two thermocouples was inserted through the top of the panel to detect LN<sub>2</sub> at 1 ft off the bottom and 3 in. from the top.

Thermocouples (type T, Cu-Constantan) were attached with Scotch tape to the outside surface of the SOFI, 6 in. from the top and 12 in. from the bottom. The temperature profile through the SOFI was measured with thermocouples embedded at various depths. In order to place the thermocouples at various depths, we cut a triangular trench through the SOFI, its apex at the aluminum plate. The thermocouples were placed along the side wall of the trench at three levels in the 0.5-in. SOFI and at four levels in the 0.9-in. SOFI. The thermocouple lead wires were routed for several inches along an approximately isothermal path to avoid temperature perturbations by heat conduction along the wires. After the lead wires were positioned, the triangular piece of foam was replaced in the trench and sealed along the edges with a thin application of RTV cement.

The test panel was mounted vertically in the environmental chamber, its bottom edge approximately 6 in. from the floor. The ambient air was sampled for dew-point temperature ( $T_{dp}$ ) measurements at four locations, two in front of the panel and two in back. Those locations were at the same height as the center of the panel and 12 in. from the panel surface. Polyflo tubing carried the sampled air to a General Eastern dew-point instrument. Thermocouples were attached near the ends of the sampling tubes to measure the ambient temperature ( $T_{amb}$ ).

### III. PROCEDURE

The initial cooling down and filling of the panel required approximately 40 min, which is comparable to the fill time expected at the launch site. Most of the thermocouples were monitored with a computerized monitoring and recording system. A few of the temperatures, including the dew-point temperatures, were read and recorded manually. During the cool-down period, the flow of LN<sub>2</sub> was carefully controlled to avoid any large pressure buildup in the panel that could have broken the seals. Once the panel was nearly full, the thermocouples on the dipstick approached the temperature of LN<sub>2</sub>, and the pressure in the panel oscillated at about 5 cps. While the panel was being filled, the internal temperature of the environmental chamber was chilled by the built-in air conditioner, as well as by the large-area heat exchangers, toward the desired operating conditions. The air conditioner was shut off once the panel was full.

During the course of a test, the desired temperatures were maintained by making small adjustments to the LN<sub>2</sub> flow rates through the panel and through the water-glycol bath of the heat exchanger. Periodically, the panel was inspected to determine the extent of frost formation. The frost thickness was measured with a metal scale scribed in 0.01-in. divisions. Samples of frost were scraped, with a razor blade, from a 3-to-5-in. × 1.5-in. area and were weighed on a triple-beam balance with a precision of 10 mg. The dimensions of the sampled area were measured and recorded.

The above scraping technique worked well for the shaved SOFI panels but might prove difficult on the rough texture of an as-sprayed panel. Therefore, we tested a technique in which the soft frost was swept from an area into a collection dish with an artist-type brush. The frost quantities measured in that way were slightly less (10-20%) than those obtained with the razor-blade scraping. The brush technique may prove useful for as-sprayed surfaces on which scraping would be difficult.

BLANK PAGE

10

## IV. RESULTS

### A. PRELIMINARY TESTS 1 THROUGH 6

Preliminary tests 1 through 6 were performed with panels sprayed in our laboratory with a foam obtained from the Aerospace shipping department. Those tests demonstrated that the large-area heat exchangers were required to maintain the desired constant-temperature and -humidity conditions.

### B. SHAVED PANEL--0.5 in. THICK

Tests 7 through 17 were conducted with a NASA-Martin Marietta-supplied SOFI-covered panel that was shaved to a thickness of  $0.5 \pm 0.03$  in. The set of data for test 12, presented in Fig. 1, indicates that both the weight and thickness of the frost increased linearly with time, starting 45 min after the panel was completely full. The test lasted 6-1/2 hr from the start of the LN<sub>2</sub> fill to the last measurement. The slope of the data gives a frost mass accretion rate of  $9.0 \times 10^{-3}$  g/cm<sup>2</sup>-hr and a thickness growth rate of 0.16 cm/hr. The density was fairly constant during the test at 0.055 g/cm<sup>3</sup> as evidenced by the linear plots of the frost mass accretion and the thickness versus time in the figure. The ratio of the frost mass accretion to the thickness determines the density.

Figure 2 shows the temperature of the SOFI surface as determined by a thermocouple held in place by a thin strip of Scotch tape. (The tape has a high conductivity compared with the SOFI and should not perturb the measurement greatly.) Once the LN<sub>2</sub> fill was started, the temperatures dropped rapidly and reached -7 to -8°C (19-18°F) about the time the LN<sub>2</sub> level indicator showed the panel to be full. The temperature held at that level for about 45 min (comparable to the time delay before the frost appearance in Fig. 1). After the 45-min delay time, frost became visible and the SOFI surface temperature began to decrease, eventually reaching -22°C (-8°F) by the end of the test. The surface temperature of the frost was not measured; therefore, the temperature drop across the frost cannot be determined. However, the SOFI temperature undoubtedly decreased because of the insulating

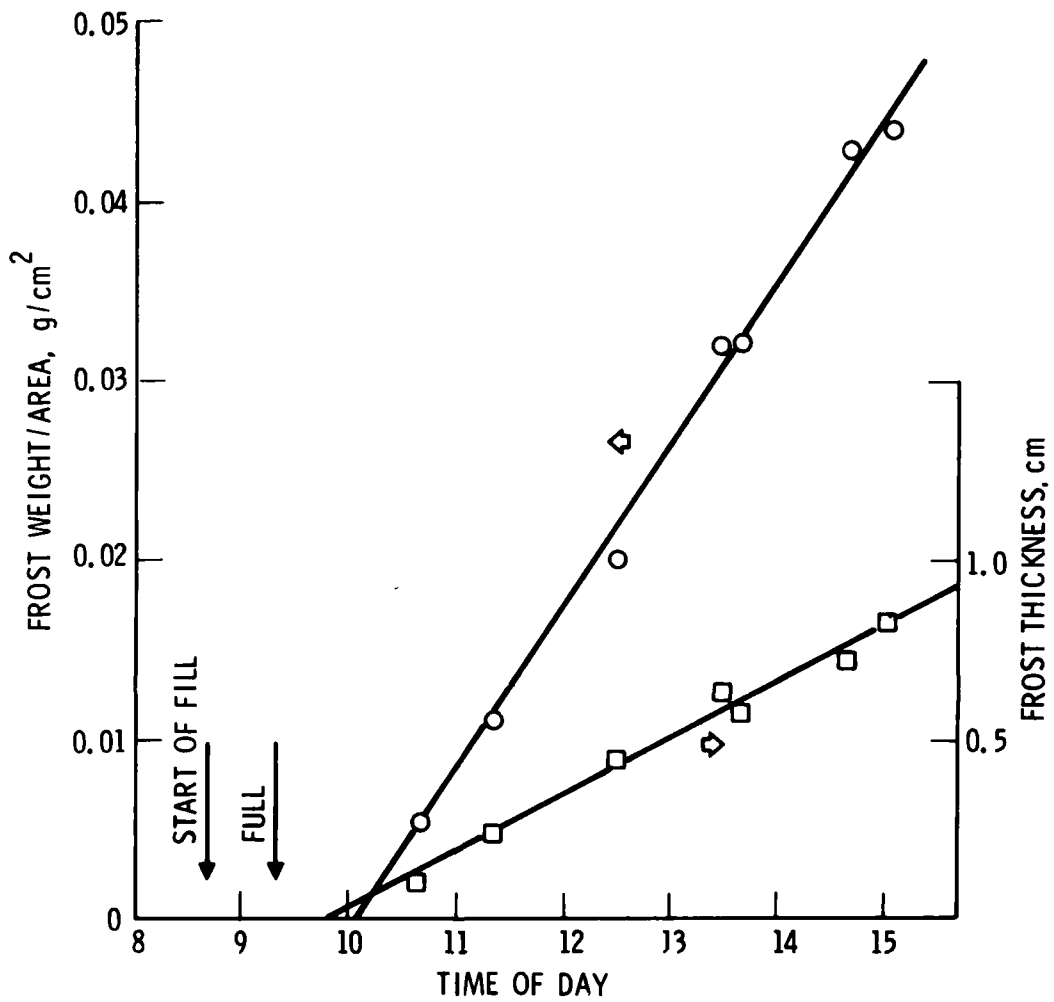


Fig. 1. Frost mass and thickness measurements for 0.5-in. SOFI in test 12.  $T_{amb}$ , 14°C; RH, 100 percent.

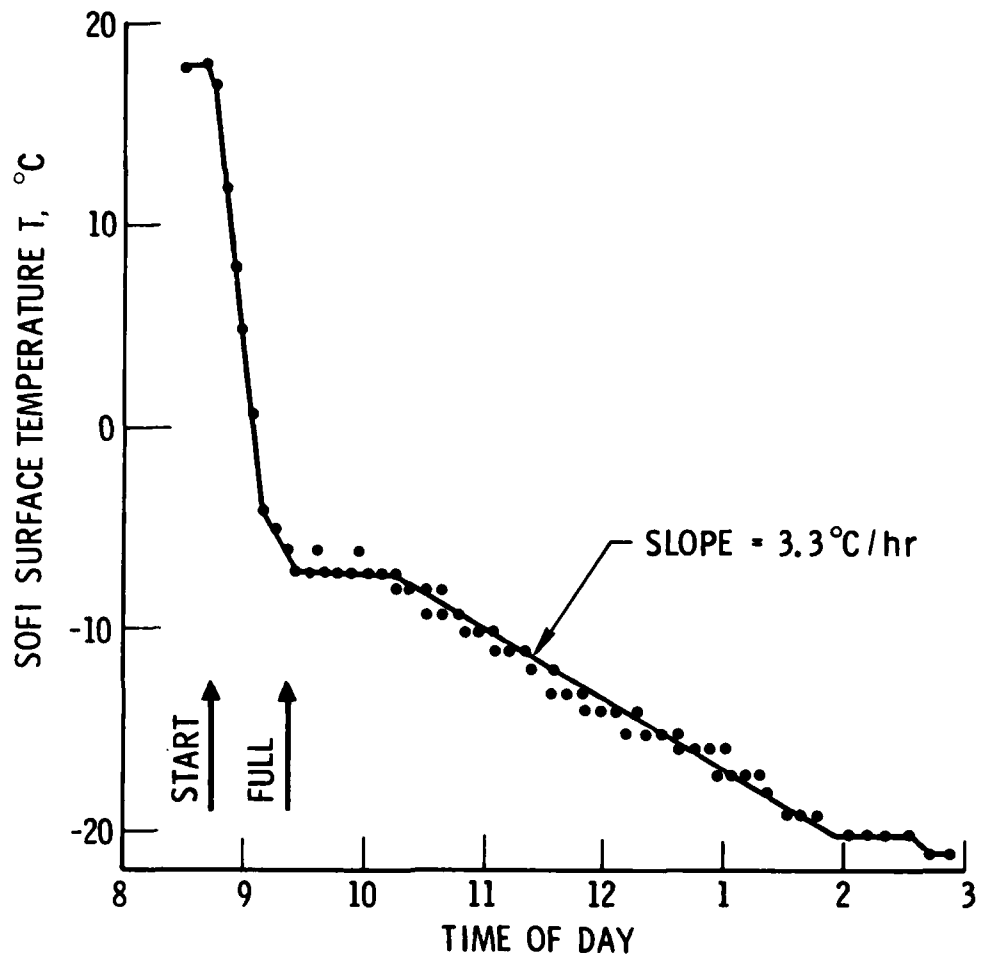


Fig. 2. Surface temperature of 0.5-in. SOFI in test 12.  $T_{amb}$ ,  $14^\circ\text{C}$ ; RH, 100 percent.



effect of the frost. The frost deposition data obtained in tests 8 through 13 are listed in Table 1.

Several special tests were conducted. Test 7 was a shakedown test; test 14 was a water-rundown test; and tests 15 and 16 were demonstrations. In test 14, conducted at ambient conditions of 15°C and 30 percent RH, water at ambient temperature was dripped onto the front of the LN<sub>2</sub>-filled panel at four equally spaced positions about 4 in. down from the top. Hypodermic needles were used to restrict the flow to about 1 drop/sec or 0.7 g/min ( $1.5 \times 10^{-3}$  lb/min) at each position. The water ran down the panel in small streams about 3 mm (1/8 in.) wide and began freezing on the lower part of the panel within 30 min after the fill was completed. The ice thickness grew almost linearly with time over the course of the 5-hr test to a final thickness of about 1.0 cm (0.4 in.), and a width of approximately 2.0 cm. The ice had an approximately semicircular cross section. The surface temperature of the ice-free portion of the panel varied between -7°C (19°F) toward the top and -11°C (12°F) toward the bottom. Toward the end of the test, the surface area of the ice was sufficiently large to freeze all of the running water. Photographs of the panel with the four icicles are presented in Fig. 3.

#### C. SHAVED PANEL--0.9 in. THICK

Tests 18 through 24 were performed with the NASA-Martin Marietta-supplied SOFI panel machined to a thickness of 0.9 in. Frost formed more slowly on this panel than on the 0.5-in.-thick panel. The frost grew linearly in mass and depth after about the same delay time (45 min) as observed for frost formation on the 0.5-in. panel; however, the measured densities tended to be higher toward the beginning of a test than toward the end. Changes in density as large as a factor of 2 were observed, and most occurred during the first 1-1/2 hr.

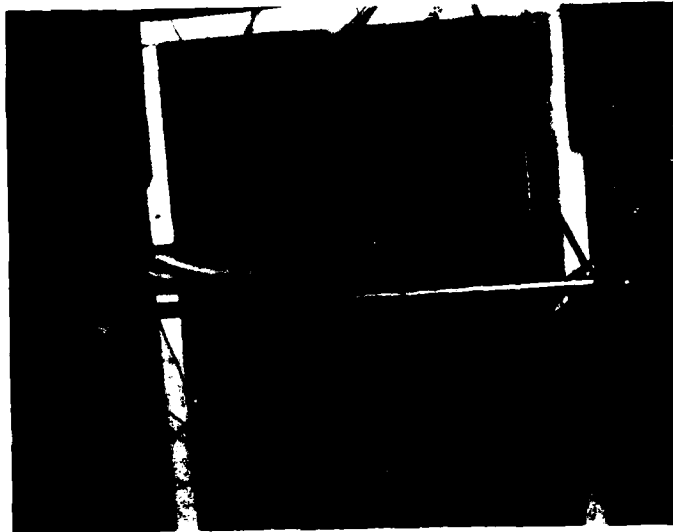
Ambient conditions, frost growth rates, densities, and surface temperatures for tests 18 through 22 are listed in Table 2. Ambient temperatures ranged from 4.6°C (40°F) to 19°C (66°F). Most of the tests were conducted between 40 and 50°F and at 97 percent RH. All of the frost densities were  $<0.1 \text{ g/cm}^3$  or  $<6 \text{ lb/ft}^3$ .

TABLE 1. EXPERIMENTAL DATA FOR 0.5-in. PANEL

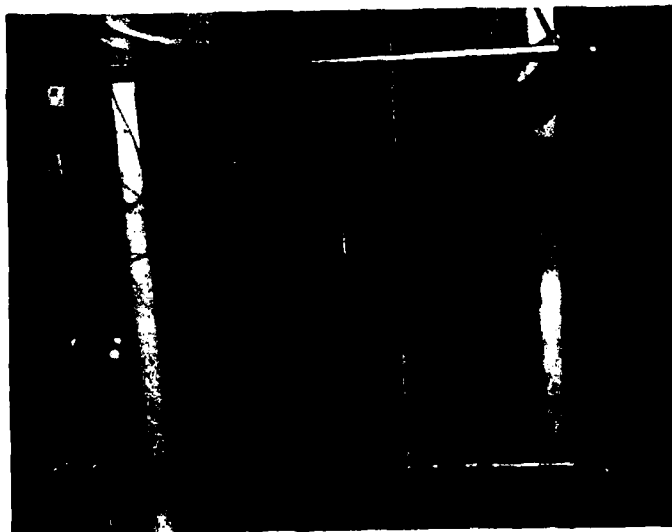
Test	$T_{amb}$		$T_{dp}$	RH	Frost Growth Rate		Density	$T_{surf}$	
	(°F)	(°C)	(°F)	(%)	(g/cm <sup>2</sup> -hr)	(cm/hr)	(g/cm <sup>3</sup> )	(°C)	(°F)
8	64	18	53	66	$6.8 \times 10^{-3}$	0.088	0.080	-8	18
9	61	16	60	100	$9.2 \times 10^{-3}$	0.150	0.060	-3	28
10	48	9	48	100	$4.9 \times 10^{-3}$	0.160	0.031	-12	10
11 <sup>a</sup>	59	15	57	95	$14 \times 10^{-3}$	0.140	0.090	-1	30
12 <sup>b</sup>	57	14	57	100	$9.0 \times 10^{-3}$	0.160	0.055	-7	19
13	55	13	34	41	$2.7 \times 10^{-3}$	0.080	0.034	-13	9

<sup>a</sup>Conducted with fan blowing at medium speed.

<sup>b</sup>Conducted with fan blowing at low speed.



(a)



(b)

Fig. 3. Ice formation in test 14: (a) upper portion of panel;  
(b) middle portion of panel.

TABLE 2. EXPERIMENTAL DATA FOR 0.9-in. PANEL

Test	T <sub>amb</sub>		RH (%)	Frost Growth Rate (g/cm <sup>2</sup> -hr)	Frost Growth Rate (cm/hr)	Density (g/cm <sup>3</sup> )	T <sub>surf</sub>		
	(°F)	(°C)					(°C)	(°F)	
18	66	19 ± 1	49 ± 1.0	54	--	--	3.2 ± 1	38 ± 2	
19A	46.5	8 ± 1	45.5 ± 1.5	97	4 ± 1 × 10 <sup>-3</sup>	0.06 ± 0.01	0.07	-6 ± 1.5	21 ± 3
19	50	10 ± 1	49 ± 1.0	97	4.6 × 10 <sup>-3</sup>	0.05	0.09	-4.0 ± 1	25 ± 2
20	40	4.6 ± 0.5	39.3 ± 0.5	97	3.2 × 10 <sup>-3</sup>	0.05 - 0.07	0.1 + 0.06	-8.5 ± 1.5	17 ± 3
21	42 ± 1	5.3 ± 1	40.8 ± 1	97	2.6 × 10 <sup>-3</sup>	~0.05 ± 0.01	0.09 + 0.06	-9.5 ± 1.5	15 ± 3
22	41.5 ± 1	5.3 ± 0.5	40 ± 1	95	2.9 × 10 <sup>-3</sup>	0.05	0.06	-10 ± 1	14 ± 2

#### D. EFFECT OF SIMULATED SOLAR RADIATION

The effect of simulated solar radiation was examined in tests 23 and 24, using the 0.9-in. panel. As depicted in Fig. 4, a 100-W light bulb mounted in a reflector/shield was placed about 7 in. from the middle of the panel. Some of the power to the bulb was lost as heat, and only part of the 100 W was radiated. However, if 100 W are assumed to radiate in all directions, then the flux on the panel directly in front of the bulb was  $\sim 0.025 \text{ W/cm}^2$  or about one-fourth the maximum solar flux of  $0.1 \text{ W/cm}^2$ .

Test 23 was run at a  $T_{\text{amb}}$  of  $9^\circ\text{C}$  ( $48^\circ\text{F}$ ) and a  $T_{\text{dp}}$  of  $45 \pm 1.5^\circ\text{F}$ . The lamp was turned on after a thin layer ( $\sim 3 \text{ mm}$ ) of frost ( $\sim 2.1 \times 10^{-3} \text{ g/cm}^2$ ) had formed. The frost melted in about 2 min and appeared to soak into the shaved SOFI surface. The accumulated frost was less than the  $14 \times 10^{-3} \text{ g/cm}^2$  required for water runoff.<sup>2</sup>

Test 24 was a repeat of test 23 except that more time was allowed for the frost to accumulate before the lamp was turned on. The frost ( $\sim 1.3 \times 10^{-2} \text{ g/cm}^2$ ) directly in front of the lamp melted within 7 min, and that in an area about 4 in. in diameter melted during the next 10 min. Some of the frost above the lamp melted because of convection currents induced by the hot lamp housing. A few drops of water moved slowly down the panel, but most of the water appeared to stay in place or diffuse into the unmelted frost.



Fig. 4. Photograph of lamp arrangement for tests 23 and 24.

## V. HEAT BALANCE MODEL PREDICTIONS

The three important variables of surface temperature ( $T_{surf}$ ), [(frost mass accumulation)/area], and thickness were measured in these simulated-ET experiments. A heat balance model relates the first two variables to the environmental conditions and physical characteristics of the SOFI. The equations are given in the Appendix, but a few remarks about the input parameters are appropriate here. The heat conduction through the SOFI depends on SOFI thermal conductivity; we have used the NASA-Martin Marietta values.<sup>1</sup> The equation for laminar, convective heat transfer to a vertical flat plate was taken from McAdams.<sup>3</sup> The mass diffusion coefficient for  $H_2O$  in air was derived from the heat transfer coefficient by the Schmidt analogy. The radiative transfer term requires the emissivities of the SOFI, the frost, and the foam insulation lining the inside walls of the environmental chamber. The emissivity of frost<sup>4</sup> is close to unity in the important infrared portion of the spectrum that dominates radiative transfer near room temperatures. The foam lining and the shaved SOFI can be expected to have large emissivities because of their small cellular structure. Even the unshaved SOFI with no open cells has a high emissivity, reported to be 0.92.<sup>5</sup> We used a value of 1.0 in the heat balance calculations; using a smaller value would have yielded a slightly lower SOFI/frost  $T_{surf}$  and a slightly larger rate of frost accumulation.

The results of the calculations for tests 8 through 13 (0.5-in. SOFI sample) are compared with the measured values in Table 3. Tests 11 and 12 were conducted with the air conditioning fan at medium and low speeds, respectively (no air conditioning). The measured frost accumulation was increased somewhat by that added convection. The calculated  $T_{surf}$  are compared with those measured in the lower half of the SOFI after the panel was filled with  $LN_2$  but before the frost began to form. The average ratios of the calculated values to the measured values for tests 8, 9, 10, and 13 were 1.13 and 1.02 for the frost growth rate and  $(T_{amb} - T_{surf})$ , respectively. This agreement is good, considering the uncertainties in the experimental data and input parameters, as well as the theoretical assumptions.

TABLE 3. COMPARISON OF EXPERIMENTAL AND CALCULATED VALUES OF FROST GROWTH RATES AND SURFACE TEMPERATURES FOR TESTS 8 THROUGH 13 (0.5-in. SOFI PANEL)

Test	Frost Growth Rate (mg/cm <sup>2</sup> -hr)			(T <sub>amb</sub> - T <sub>surf</sub> ) (°C)		
	(meas)	(calc)	(calc/meas)	(meas)	(calc)	(calc/meas)
8	6.8	6.84	1.01	26	22.6	0.87
9	9.2	9.7	1.05	19	21.3	1.12
10	4.9	6.7	1.37	21	23.0	1.10
11 <sup>a</sup>	14	--	--	16	--	--
12 <sup>a</sup>	9.0	8.3	0.92	21	21.7	1.03
13	2.7	2.96	<u>1.10</u>	26	26.1	<u>1.00</u>
Avg. Runs 8, 9, 10, and 13			1.13			1.02

<sup>a</sup>Tests affected by blower.

The measured and predicted data for tests 18 through 22 are presented for comparison in Table 4. The predicted values of (T<sub>amb</sub> - T<sub>surf</sub>) fall very close to the measured values and are well within the uncertainty of the measured values. The predicted values of the frost growth rates averaged about 12 to 13 percent higher than the measured values, although the scatter of the experimental data is somewhat large.

For the typical case, the radiation term in the heat balance equation is somewhat larger than the contributions of convective heat transfer and heat of condensation/fusion. However, all three terms are significant in the calculation of T<sub>surf</sub>. The frost condensation/fusion rate depends directly on the convective heat transfer coefficient assumed by the Schmidt analogy. Both are only weakly dependent on the difference (T<sub>amb</sub> - T<sub>surf</sub>).



TABLE 4. COMPARISON OF EXPERIMENTAL AND CALCULATED VALUES OF FROST GROWTH RATES AND SURFACE TEMPERATURES FOR TESTS 18 THROUGH 22 (0.9-in. SOFI PANEL)

Test	Frost Growth Rate (mg/cm <sup>2</sup> -hr)			(T <sub>amb</sub> - T <sub>surf</sub> ) (°C)		
	(meas)	(calc)	(calc/meas)	(meas)	(calc)	(calc/meas)
18	--	--	--	16	15.4	0.96
19A	4 ± 1	4.1	1.0	14	13.7	0.98
19	4.6	4.4	0.96	14	13.3	0.95
20	3.2	3.5	1.10	13	14.0	1.08
21	2.6	3.6	1.39	15	13.9	0.93
22	2.9	3.4	<u>1.17</u>	15	14.1	<u>0.94</u>
		Avg	1.12		Avg	0.97

24

## VI. DISCUSSION

The test results obtained with the 0.5- and 0.9-in.-thick SOFI panels indicate that fairly accurate surface temperatures and frost accumulation rates can be predicted with a heat balance model calculation. The model does not predict frost density or thickness, however. Measured and calculated frost accumulation rates are plotted in Fig. 5 and agree well except for the two points taken with the fan in operation. Although the number of measurements is small, the present data suggest that the calculations may overestimate the frost accumulation rate by about 12 percent. One source of error in the measurements may be that the convective flow down the panel was influenced by the floor, which was only 6 in. below the bottom of the panel. The cooled air had to turn and flow across the floor to make room for more air to flow across the SOFI surface. Uncertainties are introduced into the calculations by inaccuracies in the convective heat transfer coefficient recommended by McAdams,<sup>3</sup> the mass transport coefficient obtained by the Schmidt analogy from the heat transfer coefficient, the thermal conductivity values for the SOFI, and the SOFI thickness.

The most important variable affecting frost accumulation in the various tests is the humidity or the partial pressure of  $H_2O$  in the air. The measured frost accumulation rates are plotted in Fig. 6 versus  $(P_{amb} - P_{surf})$ , the difference in the partial pressure of water in the ambient air and the vapor pressure of water at the surface of the SOFI (or frost). The mass transfer coefficient depends weakly on  $\Delta T$ , the temperature difference between the ambient air and the surface, but only to the one-fourth power of that quantity.

Investigators<sup>6</sup> have predicted with some success the density of frost formation on uninsulated flat plates. Huffmann<sup>7</sup> at the University of Dayton Research Institute (UDRI) has described the frost structure with a mass diffusion model and applied that theoretical model to the present problem of frost formation on an insulated plate. Unfortunately, the initial calculations yielded frost densities between 0.2 and 0.5 g/cm<sup>3</sup>, whereas all densities

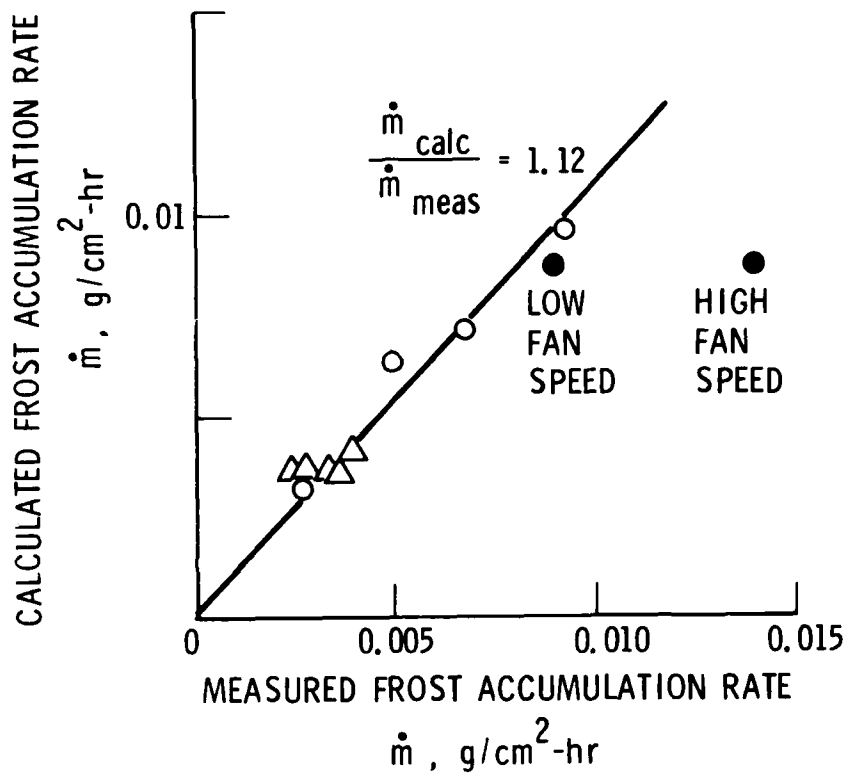


Fig. 5. Calculated frost accumulation rates versus measured frost accumulation rates. o = 0.5-in. SOFI;  $\Delta$  = 0.9-in. SOFI.

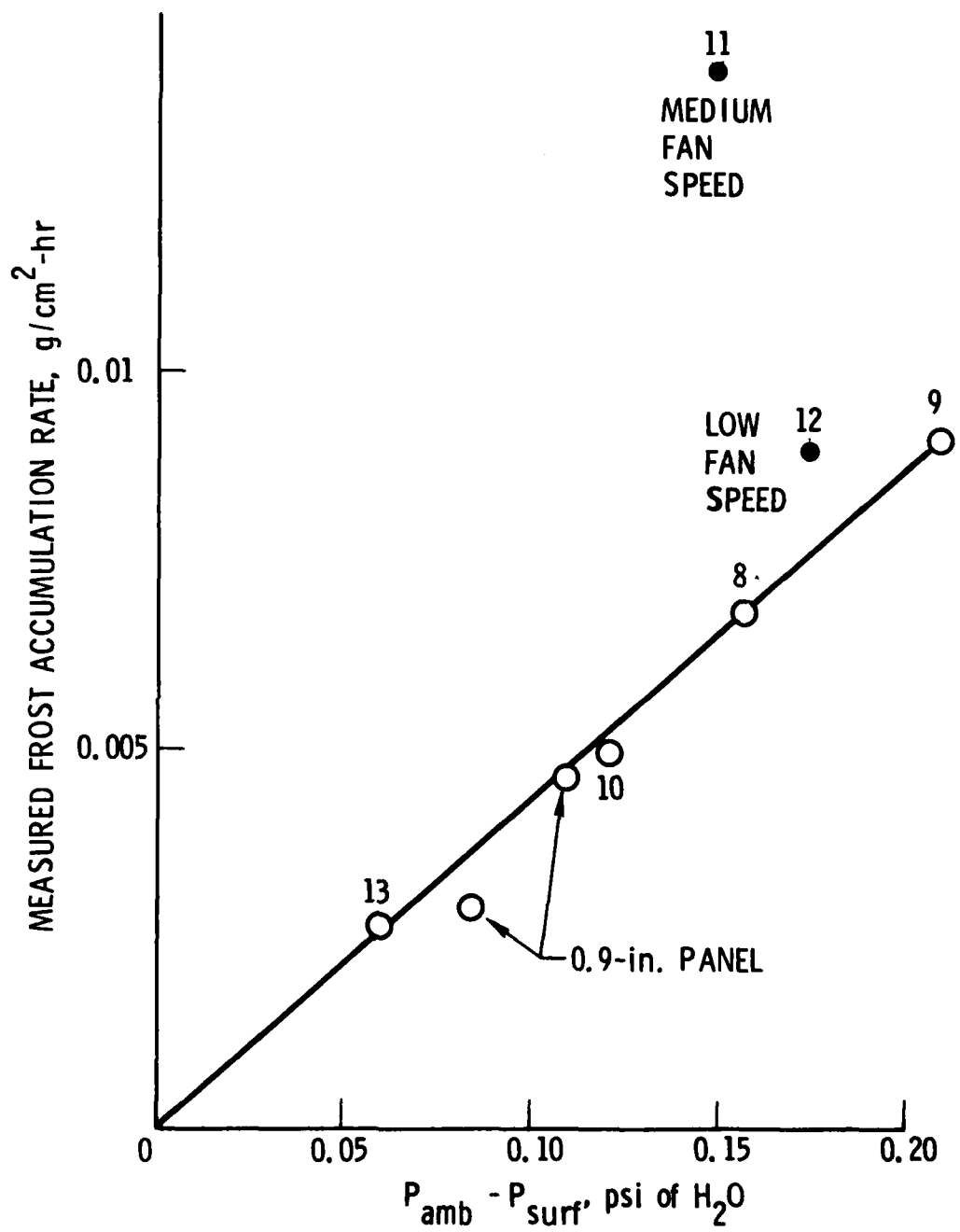


Fig. 6. Measured frost accumulation rates versus water-vapor partial pressure ( $P_{amb} - P_{surf}$ ).

are plotted versus the calculated  $T_{\text{surf}}$  in Fig. 7. They can be fitted with a straight line in the range of  $-1$  to  $-14^{\circ}\text{C}$  with a maximum deviation of  $\pm 15$  percent for any point. They correlated somewhat better with the calculated  $T_{\text{surf}}$  than with the measured ones. Extrapolations outside the present temperature range would have a high degree of uncertainty.

In this study, the frost mass and thickness grew linearly with time. In studies of uninsulated vertical plates, Nakamura (see Dietenberger et al.<sup>6</sup>), Cremers and Mehra,<sup>8</sup> and Kennedy and Goodman<sup>9</sup> have observed frost thickness growing as the square root of time, a phenomenon also observed in forced convection over uninsulated tubes.<sup>10</sup> The growth rate decreases with time as the insulating layer of frost accumulates on the otherwise uninsulated surface. The insulation serves to raise the frost surface temperature and slow the rate of water condensation/fusion. In the present case, the heat transfer rate through the SOFI remains essentially constant since the insulating effect of the frost is small compared with that of the SOFI.

The delay time observed for the start of frost formation was about 45 min for both thicknesses of SOFI. The various stages of crystal growth have been described in detail by Hayashi et al.;<sup>11</sup> also see Cremers and Mehra.<sup>8</sup> The first sign of frost was the appearance of small, needlelike crystals growing out of the surface. They began to branch out and link together, gradually forming a more uniform structure. The frost surface has a much larger effective surface area, which may facilitate frost growth. The initial limiting process to frost formation may be crystal growth on the smooth surface, with diffusion of water through the boundary layer being the limiting process only at longer times.

The running-water tests resulted in large icicles attached very firmly to the SOFI surface. They could not be dislodged by hand, and no attempt was made to pry them off the fragile SOFI. The first drops of water on the panel moved somewhat erratically down the surface because they did not wet the surface. However, once a path was formed, succeeding drops followed it. Once the column of water had begun to freeze, the drops of water ran down the ice, leaving a thin film of water to add to the icicle growth. An estimate of the

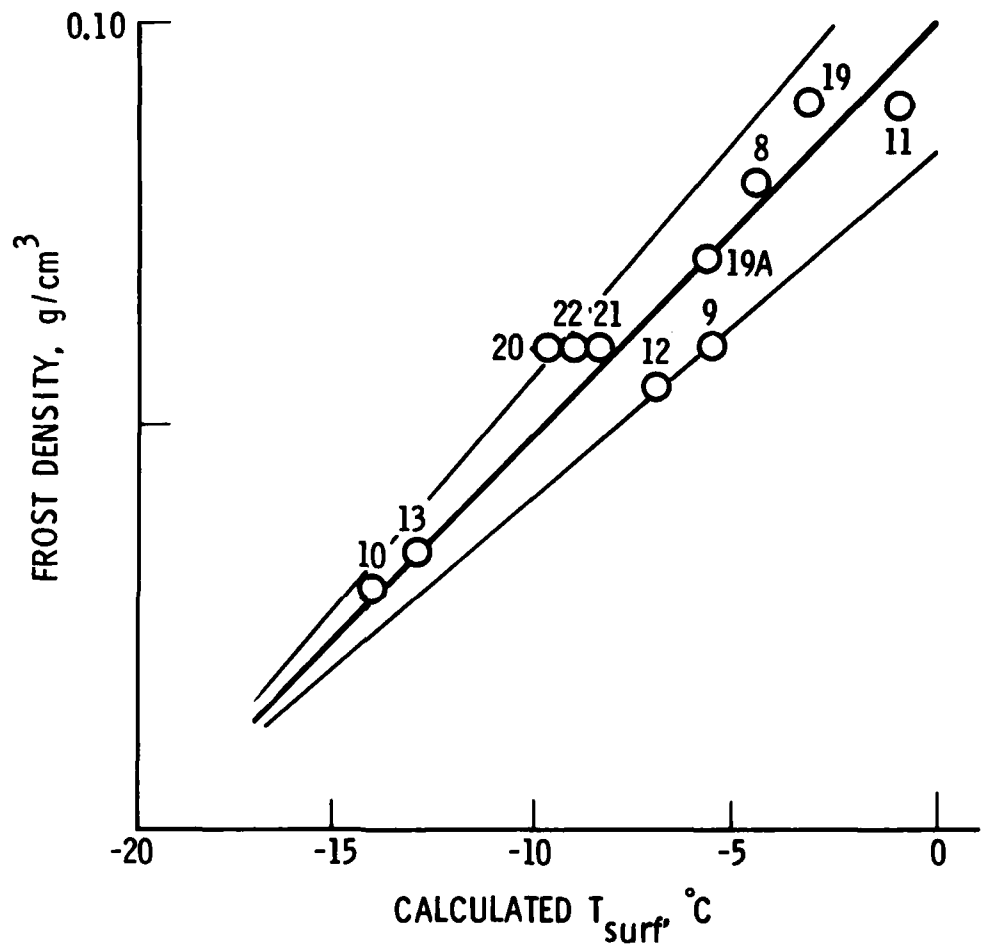


Fig. 7. Frost density versus calculated surface temperatures.

ice thickness growth rate with the heat balance model agreed fairly well with the measurements, representing the heat-transfer-limited case, in which sufficient water is assumed to be present at all times.

The results of the simulated solar experiments have been described in Section IV.D. Some of the water melted by the heat lamp adhered to the surface on which it melted, and some diffused into unmelted frost around the edges of the illumination. The test was not made quantitative with lamp intensity calibrations. However, calculations based on the nominal intensity values gave reasonably good estimates for the time required for the frost to melt. Very few drops of water formed on the machined SOFI. Water on an as-sprayed panel tends to collect in droplets more readily than on a machined SOFI surface, and melted frost might pose more of a problem on the as-sprayed SOFI by refreezing into drops of ice.

In test 12 the surface temperature of the SOFI was observed to decrease about  $3.3^{\circ}\text{C/hr}$  ( $5.9^{\circ}\text{F/hr}$ ) after the appearance of frost. This  $3.3^{\circ}\text{C/hr}$  temperature decrease represents a  $1.7\%/hr$  change in the total temperature drop of about  $190^{\circ}\text{C}$  across the SOFI, and therefore in the heat transfer rate through the SOFI. The SOFI surface temperature decreased because the frost growth served as additional insulation between the SOFI and the ambient air. During the 45 min before frost appeared,  $T_{\text{surf}}$  was approximately  $25^{\circ}\text{C}$  lower than  $T_{\text{amb}}$ . Although the frost surface temperature was not measured (the thermocouple was mounted on the SOFI surface under the frost), it would have been initially the same as the SOFI surface temperature. The  $1.7\%/hr$  decrease in the heat transfer rate through the SOFI would have been reflected in a  $1.7\%/hr$  decrease in the  $25^{\circ}\text{C}$  temperature difference between the frost surface and the ambient air. Therefore, we can conclude that the surface temperature of the frost increased  $0.43^{\circ}\text{C/hr}$ , whereas the temperature at the interface of the SOFI and the frost decreased by  $3.3^{\circ}\text{C/hr}$ . The temperature drop across the frost, therefore, increased by  $3.7^{\circ}\text{C/hr}$  ( $6.7^{\circ}\text{F/hr}$ ) as the frost thickness grew at the rate of  $0.063$  in./hr. Since the total heat transfer rate across the SOFI was calculated to be  $78$  Btu/ft<sup>2</sup>-hr, the frost thermal conductivity can be estimated to be  $0.061$  Btu/hr-ft- $^{\circ}\text{F}$  or  $0.11$  W/m-K, which is approximately equal to the theoretical and experimental values quoted in Dietenberger et al.<sup>6</sup> for



the frost temperature and density of test 12. Thermal conductivities for the other tests on the 0.5-in. panel have been calculated and plotted in Fig. 8, along with the theoretical values from Dietenberger et al.<sup>6</sup> Some uncertainty is introduced by fluctuations in the ambient temperatures during the tests. However, only one test point, that of test 8, lies out of the range of good agreement. Both the heat transfer rate and the frost thickness growth rates were smaller for the tests with the 0.9-in. SOFI panel. As a consequence, the temperature drop across the frost ( $\Delta T = qd/k$ ) was smaller in those tests, so that the frost growth did not perturb greatly the SOFI surface temperature.

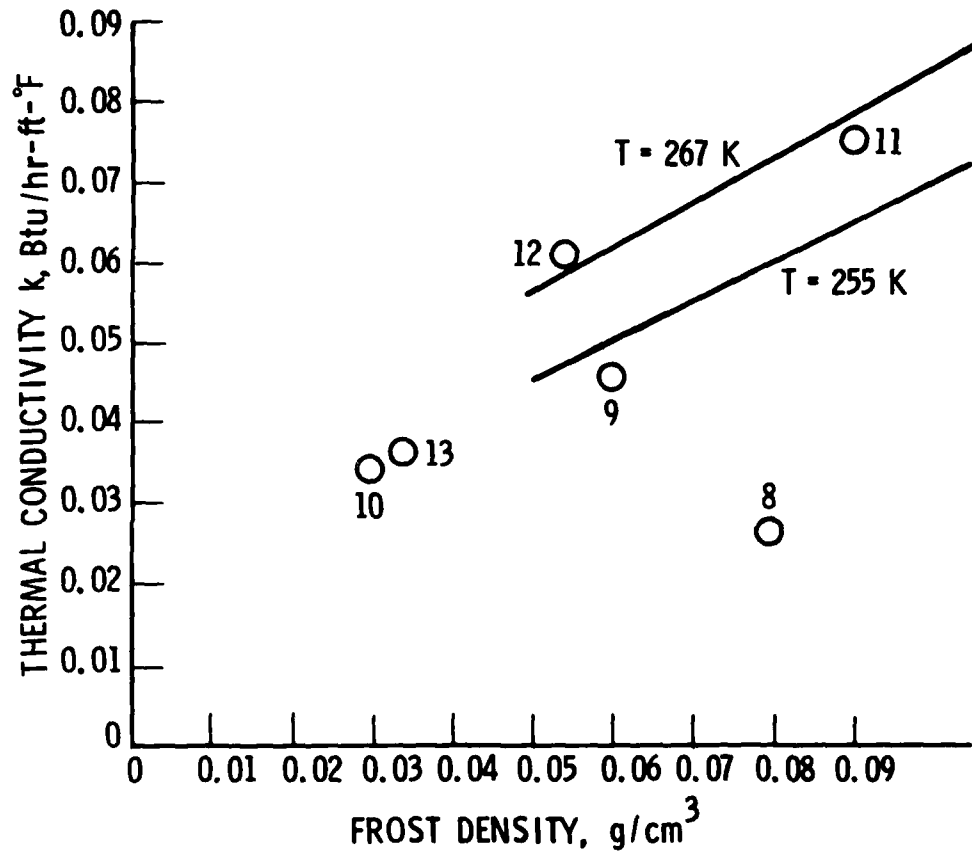


Fig. 8. Thermal conductivities of frost deduced from tests 8 through 13.

## VII. SUMMARY

Small-scale experiments have been performed with SOFI panels shaved to 0.5- and 0.9-in. thicknesses. The rear sides of the SOFI panels were cooled to  $\text{LN}_2$  temperatures; the front sides were exposed to an environmental chamber with controlled temperature and humidity. The measured rates of frost formation and the observed surface temperatures are consistent with predictions obtained with a simple heat balance model. The measured frost densities, on the other hand, were less than  $6 \text{ lb/ft}^3$ , much lower than those predicted by the UDRI frost formation model.<sup>7</sup> In a worst-case test, hard ice was observed when water was dripped down the surface of a 0.5-in.-thick,  $\text{LN}_2$ -chilled SOFI panel. A preliminary study of solar melting produced little rundown or ice. Frost densities of less than  $0.1 \text{ g/cm}^3$  ( $6 \text{ lb/ft}^3$ ) were obtained, except in the test in which water was dripped onto the surface.

Validation by the present experiments of predictions based on a heat balance model applies only to natural convection in the laminar flow regime. A large fraction of the flow on the space shuttle fuel tank will be in the turbulent regime because of the height of the tank. Larger-scale tests would be required to validate the turbulent heat transfer coefficients.

RECEIVED

34

## REFERENCES

1. Martin Marietta Briefing Charts for Orbiter Ice Debris Protection Study, Phase I Technical Interchange Meeting, Vandenberg Air Force Base, Calif. (9 July 1981).
2. J. F. Bott, The Aerospace Corporation, private communication.
3. W. H. McAdams, Heat Transmission, 2nd ed., McGraw-Hill Book Co., New York (1942).
4. H. J. Keegan and V. R. Weidner, J. Opt. Soc. Am. 56, 523 (1966).
5. L. Owens, Martin Marietta, private communication.
6. M. Dietenberger, P. Kumar, and J. Luers, Frost Formation on an Airfoil: A Mathematical Model, NASA Contractor Report 3129, University of Dayton Research Institute (UDRI), Dayton, Ohio (April 1979).
7. P. Huffman, UDRI, private communication.
8. C. J. Cremers and V. K. Mehra, J. Heat Transfer, Trans. ASME 104, 3 (1982).
9. L. A. Kennedy and J. Goodman, Int. J. Heat and Mass Transfer 17, 477 (1974).
10. H. W. Schneider, Int. J. Heat and Mass Transfer 21, 1019 (1978).
11. Y. Hayashi, A. Aoki, S. Adachi, and K. Hori, J. Heat Transfer, Trans. ASME 99, 239 (1977).

2,6

APPENDIX. HEAT BALANCE MODEL

The surface temperature  $T_{\text{surf}}$  of the SOFI can be predicted with a heat balance model in which  $q_{\text{cond}}$ , the heat conducted through the SOFI, is equated to the heat deposited on the SOFI surface by convective heating  $q_{\text{conv}}$ , radiation  $q_{\text{rad}}$ , and condensation/fusion of water vapor from the air  $q_{\text{latent}}$ , as follows:

$$q_{\text{cond}} = q_{\text{conv}} + q_{\text{latent}} + q_{\text{rad}} \quad (\text{A-1})$$

The heat conducted through the SOFI is given by

$$q_{\text{cond}} = 12 \frac{k}{\Delta X} (T_{\text{surf}} - T_{\text{cryo}}) \quad \text{Btu/ft}^2\text{-hr} \quad (\text{A-2})$$

where

$$\Delta X = \text{SOFI thickness} \quad \text{in.}$$

$$k = 0.0017 + 2.45 \times 10^{-5} T_{\text{avg}} \quad \text{Btu/hr-ft-}^\circ\text{R}$$

$$T_{\text{avg}} = \frac{(T_{\text{surf}} + T_{\text{cryo}})}{2} \quad ^\circ\text{R}$$

For example, with  $T_{\text{surf}} = 491^\circ\text{R}$  ( $26^\circ\text{F}$ ),  $T_{\text{cryo}} = 138^\circ\text{R}$ , and  $\Delta X = 1 \text{ in.}$ , then

$$k = 0.0094 \text{ Btu/hr-ft-}^\circ\text{R}$$

and

$$q_{\text{cond}} = 40 \text{ Btu/ft}^2\text{-hr}$$

The equation for convective heating is given by

$$q_{\text{conv}} = h_{\text{conv}} \Delta T \quad \text{Btu/ft}^2\text{-hr} \quad (\text{A-3})$$

where

$$\Delta T = T_{\text{amb}} - T_{\text{surf}} \quad ^\circ\text{F}$$

For laminar convection over a vertical wall,<sup>3</sup>

$$h_{\text{conv}} = 0.29 \left(\frac{\Delta T}{L}\right)^{0.25} \quad \text{Btu/ft}^2\text{-hr}$$

L = length of wall ft

$$h_{\text{conv}} = 0.22 (\Delta T)^{0.25} \quad \text{Btu/ft}^2\text{-hr for } L = 3 \text{ ft}$$

The equation for radiation is denoted as

$$q_{\text{rad}} = \sigma E (T_{\text{amb}}^4 - T_{\text{surf}}^4) \quad \text{Btu/ft}^2\text{-hr} \quad (\text{A-4})$$

where

E = emissivity = 1

$\sigma$  = Stephan-Boltzmann constant =  $1.714 \times 10^{-9}$  Btu/ft<sup>2</sup>-hr-°R<sup>4</sup>

NOTE: q can be expanded in terms of  $\Delta T$  to give

$$q_{\text{rad}} = 4\sigma E T_{\text{amb}}^3 \Delta T (1 - 3\Delta T/2T_{\text{amb}} \dots)$$



The equation for water-vapor condensation/fusion is given by

$$q_{\text{latent}} = \frac{h_{\text{conv}}}{C_{p,\text{air}}} (W_{\text{amb}} - W_{\text{surf}}) h_{fg} \quad \text{Btu/ft}^2\text{-hr} \quad (\text{A-5})$$

where

$h_{\text{conv}}$  = convective heat transfer coefficient

$C_{p,\text{air}}$  = specific heat of air at constant pressure  
= 0.24 Btu/lb-°F

$h_{fg}$  = heat of sublimation  
= 675 cal/g = 1220 Btu/lb

$W_{\text{amb}}$  = ambient water-vapor concentration, lb H<sub>2</sub>O/lb air

$W_{\text{surf}}$  = saturated water-vapor concentration  
at surface temperature, lb H<sub>2</sub>O/lb air

$W$  can be related to  $(P_{\text{amb}} - P_{\text{surf}})$  (the partial pressure of water, in psi) by

$$W = 0.042P$$

Therefore

$$q_{\text{latent}} = 47 (\Delta T)^{0.25} (P_{\text{amb}} - P_{\text{surf}}) \quad \text{Btu/ft}^2\text{-hr}$$

The mass rate of frost accumulation is written

$$\begin{aligned} \dot{m} &= 0.0388 (\Delta T)^{0.25} (P_{\text{amb}} - P_{\text{surf}}) \quad \text{lb/ft}^2\text{-hr} \\ &= \frac{q_{\text{latent}}}{h_{fg}} \quad \text{lb/ft}^2\text{-hr} \end{aligned} \quad (\text{A-6})$$

Substituting the above expressions into Eq. (A-1), one obtains the heat balance equation, with  $\Delta T$  as the unknown. Although the equation is nonlinear, a rapid convergence is obtained with an iterative procedure. A computer program written in BASIC and a sample calculation are included here (Fig. A-1). The computer program is written with the temperatures in degrees Celsius ( $^{\circ}\text{C}$ ) instead of degrees Rankine ( $^{\circ}\text{R}$ ).

>>LIST

```
10 REM PROGRAM CALLED TSURF-3 REVISED 15/JUNE/82
20 INPUT "PAMB=", P1; : PRINT "PSI";
30 INPUT " TAMB=", T1; : PRINT "DEG. C";
35 INPUT " EMISSIVITY=", E1;
40 INPUT " SOFI THICKNESS=", D3
50 C1=0.46
60 C5=39/D3
70 B=T1+273
80 C3=E1*7.2E-08*B**3
90 C4=3/(2*B)
100 D2=20 : REM FIRST GUESS FOR TAMB=TSURF
120 FOR I=1 TO 20
130 T4=T1-D2+273 : REM SURFACE TEMP CALC
140 P2=0.0886*EXP(22.46-6131/T4)
150 C6=D2**0.25
155 C2=54.4*(P1-P2)
160 D1=(C5-C2*C6)/(C1*C6+C3*(1-C4*D2))
170 IF ABS(D1-D2)<0.01 THEN 180
172 IF I=20 THEN 270
174 D2=D1
176 NEXT I
180 PRINT : PRINT
181 PRINT " PAMB = "; P1; " PSI PSURF = "; P2;
182 PRINT " PSI TAMB = "; T1; " DEGREES C"
183 T2=T1-D1
184 D=0.0219*D1**0.25*(P1-P2)
190 PRINT " TSURF="; T2; " DEGREES C DM/DT = "; D
200 @
210 PRINT " TAMB-TSURF= "; D1
220 @ : @ : @
230 @
260 STOP
270 PRINT "FAILED TO CONVERGE LAST VALUE = "; D2; "NEW VALUE="; D1
280 END
```

Fig. A-1. BASIC computer program for surface temperature.

```
>>PRINT"SAMPLE CASE TEST 12"  
SAMPLE CASE TEST 12
```

```
>>RUN  
PAMB=0.2317PSI TAMB=14DEG.C EMISSIVITY=1.0 SOFI THICKNESS=0.5
```

```
PAMB = 0.2317 PSI PSURF = 0.043911678668199 PSI TAMB = 14 DEGREES C  
TSURF=-8.290808793211 DEGREES C DM/DT = 8.9360203930777E-03
```

```
TAMB-TSURF= 22.290808793211
```

```
***260 STOP***
```

Fig. A-1. BASIC computer program for surface temperature. (Cont.)

## LABORATORY OPERATIONS

The Laboratory Operations of The Aerospace Corporation is conducting experimental and theoretical investigations necessary for the evaluation and application of scientific advances to new military space systems. Versatility and flexibility have been developed to a high degree by the laboratory personnel in dealing with the many problems encountered in the nation's rapidly developing space systems. Expertise in the latest scientific developments is vital to the accomplishment of tasks related to these problems. The laboratories that contribute to this research are:

Aerophysics Laboratory: Launch vehicle and reentry aerodynamics and heat transfer, propulsion chemistry and fluid mechanics, structural mechanics, flight dynamics; high-temperature thermomechanics, gas kinetics and radiation; research in environmental chemistry and contamination; cw and pulsed chemical laser development including chemical kinetics, spectroscopy, optical resonators and beam pointing, atmospheric propagation, laser effects and countermeasures.

Chemistry and Physics Laboratory: Atmospheric chemical reactions, atmospheric optics, light scattering, state-specific chemical reactions and radiation transport in rocket plumes, applied laser spectroscopy, laser chemistry, battery electrochemistry, space vacuum and radiation effects on materials, lubrication and surface phenomena, thermionic emission, photosensitive materials and detectors, atomic frequency standards, and bioenvironmental research and monitoring.

Electronics Research Laboratory: Microelectronics, GaAs low-noise and power devices, semiconductor lasers, electromagnetic and optical propagation phenomena, quantum electronics, laser communications, lidar, and electro-optics; communication sciences, applied electronics, semiconductor crystal and device physics, radiometric imaging; millimeter-wave and microwave technology.

Information Sciences Research Office: Program verification, program translation, performance-sensitive system design, distributed architectures for spaceborne computers, fault-tolerant computer systems, artificial intelligence, and microelectronics applications.

Materials Sciences Laboratory: Development of new materials: metal matrix composites, polymers, and new forms of carbon; component failure analysis and reliability; fracture mechanics and stress corrosion; evaluation of materials in space environment; materials performance in space transportation systems; analysis of system vulnerability and survivability in enemy-induced environments.

Space Sciences Laboratory: Atmospheric and ionospheric physics, radiation from the atmosphere, density and composition of the upper atmosphere, auroras and airglow; magnetospheric physics, cosmic rays, generation and propagation of plasma waves in the magnetosphere; solar physics, infrared astronomy; the effects of nuclear explosions, magnetic storms, and solar activity on the earth's atmosphere, ionosphere, and magnetosphere; the effects of optical, electromagnetic, and particulate radiations in space on space systems.